EFFECT OF WALL CURVATURE WITH WAVY DOWNFLOW OF A THIN LAYER OF VISCOUS LIQUID

Yu. Ya. Trifonov

UDC 532.516

Different wave regimes are considered for downflow of a thin layer of viscous liquid over the outer and inner surfaces of a vertical cylinder. A simple set of evolutionary equations is derived on the basis of the integral method from Navier–Stokes equations and the linear stability of its trivial solution is studied. Different linear solutions for the set obtained are calculated within the depth of the instability region by means of numerical methods. In contrast to case of downflow over a vertical plane where as a single external parameter there was $Z^{-1} = (Re^{11}/81Fi)^{1/6}$ (Re is Reynolds number, $Fi = (\sigma/\rho)^3/g\nu^4$ is film number), in considering wall curvature there are additional parameters: wall curvature R^{-1} and Fi. The effect of all of the parameters on nonlinear wave characteristics is analyzed. It is demonstrated that an increase in wall curvature R^{-1} always intensifies wave processes, and with flow over an inner cylinder wall of quite small radius a "catastrophic" growth in wave amplitude with movement within the region of linear instability is observed in calculations.

1. Two-dimensional downflow is considered for a layer of viscous incompressible liquid (Fig. 1) over the outer (a) and inner (b) surfaces of a vertical cylinder. In future we limit ourselves to studying the evolution of only long-wave disturbances of the free surface of the layer for which we introduce a small parameter $\varepsilon = h_*/L$, where h_* is scale of film thickness (for example, average thickness), L is longitudinal scale of disturbances (for example, wavelength). By considering a different scale for movement along coordinates r and z, and making the Navier–Stokes equations and boundary conditions dimensionless, after discarding terms $O(\varepsilon)$ in the range $\varepsilon \ll Re \leq 1/\varepsilon$ we obtain

$$\frac{\partial u}{\partial t} + v\frac{\partial u}{\partial r} + u\frac{\partial u}{\partial z} = -\frac{1}{\rho}\frac{\partial p}{\partial z} + g + \nu\left(\frac{\partial^2 u}{\partial r^2} + \frac{1}{r}\frac{\partial u}{\partial r}\right),$$
$$\partial p/\partial r = 0,\ \partial(ur)/\partial z + \partial(vr)/\partial r = 0,\ u = v = 0,\ r = R,\ \partial u/\partial r = 0, \qquad (1.1)$$
$$r = R \pm h(z,\ t),$$
$$p = p_0 - \sigma\left(\mp\frac{1}{R \pm h} + \frac{\partial^2 h}{\partial z^2}\right).$$

Here u is velocity along axis z; v is velocity in the direction of axis r; p is pressure; p_0 is atmospheric pressure; g is acceleration due to gravity; ρ is liquid density; ν is kinematic viscosity; R is cylinder radius; h is instantaneous film thickness; σ is surface tension coefficient. Upper and lower symbols in (1.1) and in future relate to the case of downflow over the outer cylinder wall (flow over a wire) or an inner wall (flow in a tube), respectively.

We note that retention in the boundary condition of a term with capillary pressure $\sim\partial^2 h/\partial z^2$ is correct if a liquid with large $Fi \sim Re^5/\varepsilon^6$ is studied, and this is fulfilled for the majority of experimental liquids considered [1].

It is easy to write the solution of Eqs. (1.1) appropriate with any liquid flow rates and relating to waveless downflow:

$$u = \frac{gR^2}{4\nu}\left[1 - \left(\frac{r}{R}\right)^2 + 2\left(1 \pm \frac{h_0}{R}\right)^2 \ln\frac{r}{R}\right],\ v = 0,$$
$$p = p_0 - \sigma\left(\mp\frac{1}{R \pm h_0}\right),\ h = h_0 = \mathrm{const}.$$

The search for other solutions of Eqs. (1.1) requires drawing on considerable computing resources, and in this work for simplicity we use the assumption of self-modeling for the longitudinal profile of velocity:

Novosibirsk. Translated from Prikladnaya Mekhanika i Tekhnicheskaya Fizika, No. 5, pp. 56-65, September-October, 1992. Original article submitted June 26, 1991.

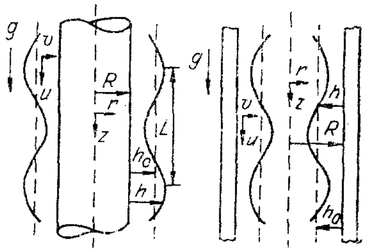

Fig. 1

$$u(r,z,t)=\pm\frac{q(z,t)}{Rf_{\pm}(h(z,t)/R)}\left[1-\left(\frac{r}{R}\right)^2+2\left(1\pm\frac{h(z,t)}{R}\right)^2\ln\frac{r}{R}\right],$$
$$q(z,t)=\pm\frac{1}{R}\int_R^{R\pm h} ur\,dr, \tag{1.2}$$
$$f_{\pm}(h/R)=1/4-(1\pm h/R)^2+(1\pm h/R)^4(3/4-\ln(1\pm h/R)).$$

This profile satisfies the conditions of attachment at the wall and quality to zero of the tangential stress at the free boundary. In addition, for flow with a smooth free boundary (1.2) it is converted into an accurate solution of the Navier–Stokes equations. At the limit $R\to\infty$ (flow over a vertical wall) from (1.2) it follows that

$$u(\delta,z,t)=\frac{3q(z,t)}{h(z,t)}\left(\frac{\delta}{h(z,t)}-\frac{\delta^2}{2h^2(z,t)}\right)$$

(δ is transverse coordinate read from the wall).

For flow over a vertical plane there are both experimental [2] and theoretical [3] works which demonstrate the correctness of assuming self-modeling of the longitudinal velocity profile. The validity of the integral approach is also demonstrated convincingly in [4-6] where on the basis of it different nonlinear waves are calculated which agree quantitatively with observations in experiments [1, 7].

For long waves in the case of flow over a vertical cylinder assumption (1.2) is also quite reasonable. From a physical point of view the validity of relationship (1.2) may be established by comparing the results calculated by means of it with experimental or calculated results found on the basis of Navier–Stokes equations.

From (1.1) and (1.2) by integration along axis r [from R to $R\pm h(z,t)$] it is easy to obtain

$$\pm\frac{\partial q}{\partial t}\pm 1{,}2\frac{\partial}{\partial z}\left(\frac{q^2}{h}f_1\left(\pm\frac{h}{R}\right)\right)=\left(g+\frac{\sigma}{\rho}\left(\frac{1}{(R\pm h)^2}\frac{\partial h}{\partial z}+\frac{\partial^3 h}{\partial z^3}\right)+\right.$$
$$\left.+\frac{3\nu q}{h^3 f(\pm h/R)}\right)\left(\pm h+\frac{h^2}{2R}\right),$$
$$\frac{\partial h}{\partial t}+\frac{R}{R\pm h}\frac{\partial q}{\partial z}=0, \tag{1.3}$$
$$f=3(1/4-y^2+y^4(3/4-\ln(y)))/4(y-1)^3,\ y=1\pm h/R,$$
$$f_1=(y-1)\left(-\frac{1}{6}+\frac{5}{4}y^2-\frac{5}{2}y^4+\frac{17}{12}y^6+2y^4\ln(y)-3y^6\ln(y)+\right.$$
$$\left.+2y^6\ln^2(y)\right)\Big/\left(1{,}2\left(\frac{1}{4}-y^2+y^4\left(\frac{3}{4}-\ln(y)\right)\right)^2\right).$$

In deriving (1.3) use is also made of the kinematic condition at the free surface

$$\pm v=\partial h/\partial t+u\partial h/\partial z,\ r=R\pm h(z,t).$$

At the limit $R\to\infty$ ($f_1\to 1$, $f\to -1$) set (1.3) is converted into a set of Shkadov equations [8].

We note that a similar integral approach was used in [9] in studying downflow of a magnetic liquid over the outer surface of a vertical cylinder. In the absence of a magnetic field the set of equations provided in [9] is a special case of set (1.3).

In this work calculation of the instability of the trivial solution and calculations of different nonlinear wave regimes were carried out on the basis of Eqs. (1.3) whose solution corresponding to waveless downflow is written in the form

$$h = h_N,\ q = q_N = -\frac{gh_N^3}{3\nu} f(\pm h_N/R).$$

For downflow over a vertical plane this is the well-known Nusselt relationship. In order to study the stability of waveless downflow we place in set (1.3) the relationships

$$h = h_N + h',\ q = q_N + q',\ (h',\ q') \sim \exp\left[i\alpha(z - \gamma t)\right]$$

($\alpha = 2\pi/\lambda$, λ is the disturbance wavelength). By linearizing it with respect to h', q', it is easy to find that

$$\begin{gathered} -\gamma^2 y_N + \gamma\left(2{,}4\frac{q_N}{h_N} y_N f_1(y_N) \mp \frac{3\nu y_N R\left(y_N^2 - 1\right)}{2i\alpha h_N^3 f(y_N)}\right) \pm \\ \pm\frac{\sigma R\left(y_N^2 - 1\right)}{2\rho}\alpha^2 - \left(1{,}2\frac{q_N^2}{h_N^2} f_1(y_N) \mp 1{,}2\frac{q_N^2}{h_N R}\frac{df_1}{dy}\bigg|_{y=y_N} \pm \frac{\sigma}{\rho R}\frac{y_N^2 - 1}{2y_N^2}\right) \pm \\ \pm\frac{3\nu q_N R\left(y_N^2 - 1\right)}{2i\alpha h_N^3 f^2}\left(\frac{3f(y_N)}{h_N} \pm \frac{1}{R}\frac{df}{dy}\bigg|_{y=y_N}\right) = 0,\ y_N = 1 \pm h_N/R. \end{gathered} \tag{1.4}$$

Then parameter α is assumed to be real and (1.4) serves in order to determine complex increment γ. If $\mathrm{Im}(\lambda) > 0$, then the corresponding disturbance increases with time, and if $\mathrm{Im}(\gamma) < 0$, then waveless flow is stable.

In dimensionless variables the characteristics of neutral disturbances ($\mathrm{Im}(\gamma) = 0$, $c_{neut} = \mathrm{Re}(\gamma)$) obtained from (1.4) may be written in the form

$$\begin{gathered} \left(\alpha_{\text{neut}}^*\right)^2 = \pm\frac{2}{\mathrm{We}\, R^*\left(y_N^2 - 1\right)}\left(y_N c_{\text{neut}}^{*2} - 2{,}4\frac{1}{h_N^*} y_N f_1 c_{\text{neut}}^* + 1{,}2\frac{f_1}{h_N^{*2}} \mp\right. \\ \left.\mp\frac{1{,}2}{h_N^* R^*}\frac{df_1}{dy}\bigg|_{y=y_N} \pm \mathrm{We}\frac{y_N^2 - 1}{2y_N^2 R^*}\right), \\ c_{\text{neut}}^* = \frac{1}{y_N f(y_N) h_N^*}\left(3f(y_N) \pm \frac{h_N^*}{R^*}\frac{df}{dy}\bigg|_{y=y_N}\right),\ 1 + h_N^{*3} f(y_N) = 0. \end{gathered} \tag{1.5}$$

Here $h_N^* = h_N/h^*$; $c^* = \gamma h^*/q_N$; $R^* = R/h^*$; $\mathrm{Re} = q_N/\nu$; $\mathrm{We} = (\sigma/\rho)h^*/q_N^2 = (3\mathrm{Fi}/\mathrm{Re}^5)^{1/3}$; $\mathrm{Fi} = (\sigma/\rho)^3/g\nu^4$; $\alpha^* = \alpha h^*$; $h^* = (3\nu q_N/g)^{1/3}$. Disturbances with $\alpha^* < \alpha_{neut}^*$ increase with time, but with $\alpha^* > \alpha_{neut}^*$ they fade.

Numerical analysis of Eqs. (1.5) showed that with any values of parameters We and R^* there is a neutral disturbance and increasing modes. With $R^{*-1} = 0$ (downflow over a vertical plane) it follows from (1.5) that $\alpha_{neut}^* = \sqrt{3/\mathrm{We}}$, $c_{neut}^* = 3$, $h_N^* = 1$. With an increase in wall curvature for downflow both over a wire and over the inner surface of a cylinder there is expansion of the region nonlinear instability (i.e., shorter wave modes become increasing modes), and the higher the We (small Re for an immobile liquid), the more marked is the deviation from the dependence $\sqrt{3/\mathrm{We}}$. For the same value of R^* with any We the region of increasing disturbances for flow over the inner wall of a cylinder is broader than the similar region for flow over a wire. In contrast to downflow over a vertical plane, for flow over a cylindrical surface neutral curves with $\mathrm{Re} \to 0$ tend toward a finite value.

In order to evaluate the correctness of the long-wave approximation used above, as a scale for longitudinal movement it is possible to take the wavelength of a neutral disturbance, then it is easy to see that $\varepsilon \approx \alpha_{neut}^*/2\pi$. As calculations showed, in the range $0 \le R^{*-1} \le 0.2$, $5 \le \mathrm{We} < \infty$ the value of ε does not exceed 0.1.

As follows from (1.5), the thickness of a waveless film h_N^* and the phase velocity of neutral disturbances c_{neut}^* are only functions of the dimensionless cylinder radius R^*. In the range $0 \le R^{*-1} \le 0.2$ the dependences $h_N^*(R^{*-1})$ and $c_{neut}^*(R^{*-1})$ are almost linear functions and for downflow over a wire they decrease with an increase in wall curvature ($h_N^* \cdot (R^{*-1}) \le 1$, $c_{neut}^*(R^{*-1}) \le 3$), but for flow over the inner surface of a cylinder they increase ($h_N^*(R^{*-1}) \ge 1$, $c_{neut}^*(R^{*-1}) \ge 3$).

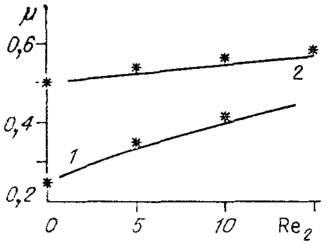

Fig. 2

Given in Fig. 2 is a comparison for curves for neutral stability calculated by Eqs. (1.5) (lines) with data in [10] (marked by asterisks) where these dependences were calculated by means of asymptotic expansion of the solution for Navier–Stokes equations with respect to the long-wave parameter. In Fig. 2 the variables are dimensionless similar to [10] and $\mu = 2\pi h_N/\lambda$, $Re_2 = u_{max}h_N/\nu$ (u_{max} is free surface velocity), $R_2 = R/h_N$. Line 1 relates to downflow over a wire with $R_2 = 3$, $We_2 = \sigma/(\rho g h_N^2) = 100$, 2 relates to downflow within a tube with $R_2 = 3$, $We_2 = 100$. The comparison demonstrates the good quantitative agreement which to a certain extent confirms the correctness of the integral approach used.

In order to calculate periodic steady-state traveling solutions of Eq. (1.3) [$q = q(z - ct)$, $h = h(z - ct)$, c is phase velocity] of finite amplitude it is convenient to rewrite it in dimensionless form

$$- c^* \frac{dq^*}{d\xi^*} + 1{,}2 \frac{d}{d\xi^*}\left(\frac{q^{*2}}{h^*} f_1(y)\right) = \left(\pm \mathrm{We}\left(\frac{1}{(R^* \pm h^*)^2}\frac{dh^*}{d\xi^*} + \frac{3}{\mathrm{We}}\frac{d^3h^*}{d\xi^{*3}}\right) + \right.$$
$$\left. + Z\left(\pm 1 \pm \frac{q^*}{h^{*3} f(y)}\right)\right)\left(\pm h^* + \frac{h^{*2}}{2R^*}\right), \tag{1.6}$$
$$q^* = 1 \pm c^*\left(\pm h^* + \frac{h^{*2}}{2R^*} - \left\langle \pm h^* + \frac{h^{*2}}{2R^*}\right\rangle\right), \; y = 1 \pm \frac{h^*}{R^*},$$

here $\xi^* = \sqrt{3/\mathrm{We}}(\xi/h_s)$; $\xi = z - ct$; $h^* = h/h_s$; $R^* = R/h_s$; $q^* = q/q_0$; $c^* = ch_s/q_0$; $h_s = (3\nu q_0/g)^{1/3}$; $\mathrm{We} = (3\mathrm{Fi}/\mathrm{Re}^5)^{1/3}$; $Z = (81\mathrm{Fi}/\mathrm{Re}^{11})^{1/6}$; $\mathrm{Re} = q_0/\nu$; $q_0 = \langle q\rangle = (1/\lambda)\int^{\lambda} q(\xi)\,d\xi$; λ is the wavelength.

By excluding q(ξ) (here and in the future we omit the dimensionless symbol) from the first equation of (1.6), in order to determine h(ξ) and c we find a unique equation. In order to calculate h(ξ) we use expansion into a Fourier series:

$$h(\xi) = \sum_{-\infty}^{\infty} H_n \exp[i\alpha n\xi], \; \overline{H}_{-n} = H_n \tag{1.7}$$

(a line means complex conjugation).

By considering the first N/2 harmonics in (1.7) and by substituting in the equation it is easy to obtain a set of N + 1 nonlinear algebraic equations for determining the two real (H_0, c) and N/2 complex ($H_1, \ldots, H_{N/2}$) unknowns. In view of the invariance of Eqs. (1.6) with respect to transformation $\xi^* \to \xi^* + \mathrm{const}$ it is possible to consider the phase of one of the harmonics in (1.7) known, for example, $\mathrm{Image}(H_1) = 0$.

The Newton method is used for numerical calculation of the algebraic set. A pseudospectral method and a procedure for rapid Fourier transformation are used in order to calculate the Fourier harmonic of nonlinear terms in (1.6).

In cutting off series (1.7) in the calculations it was necessary to satisfy the conditions $|H_{N/2}|/\sup|H_n| < 10^{-3}$. For this the value of N in relation to α, Re, and Fi was varied within the limits from 16 to 128.

2. In Eqs. (1.6) there are three internal parameters: R, Z, We, or R, Fi, Re. We note that for downflow over a vertical plane ($R \to \infty$) in (1.6) only one parameter Z remains. Apart from external parameters in the problem there is one more internal parameter, i.e., wave number α. External parameters have a clear physical meaning. In order to interpret the internal parameter we turn to experiments in [1, 11]. In both [11] and [1, 7] without special

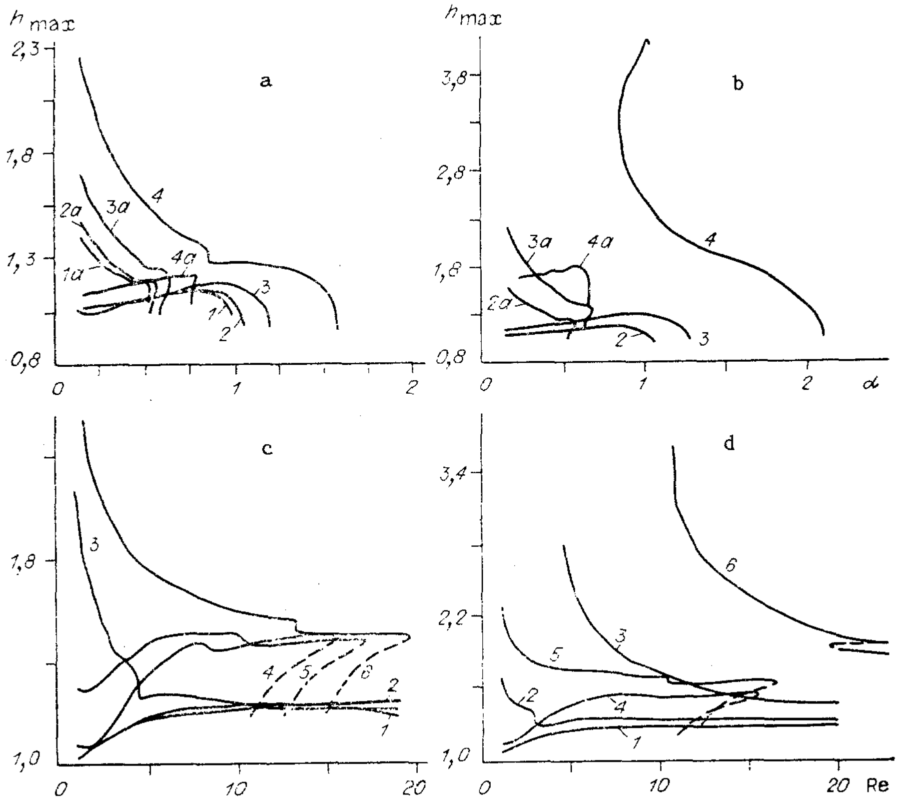

Fig. 3

organization of the flow surface films were covered by three-dimensional waves in both space and time. With imposition of pulses which are small in amplitude on liquid flow rate in the input flow cross section and with careful removal of spatial roughness for the wall a section is observed in annular waves regular in space and steady-state waves traveling with time. Wave periodicity was determined by the frequency of imposed pulsations, but the amplitude did not depend on the amplitude of the imposed vibrations. By changing frequency ω ($\omega = c/\lambda = \alpha c/2\pi$), it is possible to see different wave regimes for a given liquid flow rate. In [11] authors separated the waves observed into two classes, i.e., periodic and solitary waves.

In theory the main difficulty in finding a solution of Eqs. (1.6) by the Newton method involves determining a good initial approximation. By using calculated results for waves for a vertical wall [4, 5] and moving with respect to parameters α, R, Fi, Re, we calculated wave regimes in a wide range of external parameters down to very small values of α (~0.1). Calculated results are presented in Figs. 3-5. Since there are many parameters in the problem, it is difficult to carry out a detailed study and the main attention is devoted to qualitative differences between wavy downflow over a vertical plane and over the inner and outer walls of a vertical cylinder.

The dependences of maximum thickness of a wavy film h_{max} on a number α for downflow over a wire and over the inner wall of a cylinder are presented in Fig. 3a, b, respectively. Here values of Re and Fi are fixed: Re = 4, $Fi^{1/11} = 6.8$. Lines 1, 1a-4, 4a relate to $R^{-1} = 0$, 0.05, 0.1, 0.2. Lines 1, 1a in Fig. 3a relate to downflow over a vertical plane. Wave solutions in this case branch out from trivial solution h = 1 at point α = 1 and continue into the region of linear instability of waveless flow (α < 1) [8]. Down to α ≈ 0.55 the wave profile of thickness is close to sinusoidal and with α → 0 it is converted into a sequence of solitary waves, i.e., negative solitons [12]. The comparison carried out in [5, 6] of experimental results showed that waves of a given family (in future the first family of waves) correspond quantitatively to periodic regimes observed in experiments. Long waves of this family are unstable [5] and they differ qualitatively from those observed in long-wave experiments.

It is noted in [13, 14] that apart from the first family of waves there are many different single-parameter families of solutions which develop from both the first family and from each other as a result of different bifurcations. Among the new families there appears to be only one family separate in the sense of stability [14] (in future the second family) which branches from the first as a result of double period bifurcation. Line 1a in Fig. 3a relates to the second family, and as shown in [4-6] the regime of this family describes quantitatively long waves close to a sequence of solitary waves observed in experiments.

With downflow over the outer surface of a cylinder similar to downflow over a vertical plane there exist at a minimum two families of wave solutions which have at the limit with $\alpha \to 0$ negative solitary waves ($|h_{max} - \langle h \rangle| < |h_{min} - \langle h \rangle|$, $\langle h \rangle$ is average wave thickness over the length) and positive waves ($|h_{max} - \langle h \rangle| > |h_{min} - \langle h \rangle|$). The first branch branches from the trivial solution (lines 2-4 in Fig. 3a), and the second (lines 2a-4a in Fig. 3a) branches from the corresponding solution for the first family with doubling of the spatial period. The asymptotic behavior of wave characteristics of solutions for these two branches differs markedly. Thus, with small α values of h_{max} for solutions of the branch which has at the limit with $\alpha \to 0$ positive solitary waves (lines 1a-3a, 4 in Fig. 3a) increase with a reduction in α, and values of h_{max} for solutions of the branch which has at the limit "negative" solitary waves (lines 1-3, 4a in Fig. 3a) decrease. It is also noted that values of h_{max} and other wave characteristics change in a markedly smaller range from the branch which has at the limit "negative" solitary waves, than for values of these characteristics for the branch which has at the limit positive solitary waves.

There is a single qualitative difference in downflow over a wire of quite small radius from downflow over a plane. Considering curvature the branch which has at the limit a positive solitary wave may branch immediately from the trivial solution (line 4 in Fig. 3a) in contrast to downflow over a plane where this branch originates from the wave of the first family.

With downflow over the inner surface of a vertical cylinder some qualitative similarity is also observed with downflow over a plane, but the difference is more marked. Thus, for values of $R^{-1} < R_{cr}^{-1}(\mathrm{Re}, \mathrm{Fi})$ there are two branches of solutions which have at the limit with $\alpha \to 0$ a positive solitary wave (lines 2a, 3a in Fig. 3b) and a negative wave (lines 2, 3, 4a in Fig. 3b). For $R^{-1} > R_{cr}^{-1}$ the branch with branches from the trivial solution ceases to exist for $\alpha < \alpha_{cr}$ (line 4 in Fig. 3b). The wave amplitude on approaching point α_{cr} decreases rapidly and it takes a considerably larger number of harmonics in series (1.7) in order to satisfy the cutting-off conditions. Further advance along line 4 in Fig. 3b is limited by the computing possibilities. The value of h_{max} is close to the value of tube radius, and the minimum thickness value is close to zero.

Thus, from the results presented in Figs. 3a and b it is possible to conclude that for downflow of a liquid film over the outer surface of a vertical cylinder and over an inner surface of quite small curvature there exist at a minimum two branches differing markedly with respect to the properties of the solutions whose regions for existence intersect with comparatively small wave numbers. One of the branches at the limit $\alpha \to 0$ is converted into a sequence of solitary negative waves which for flow over a vertical surface were unstable [5]. We shall not consider further such solutions for a cylinder of finite radius in view of their instability.

Presented in Fig. 3c, d for some wave regimes with fixed α are dependences of maximum film thickness h_{max} on Re for downflow over a wire and over the inner surface of a cylinder, respectively. Here $\mathrm{Fi}^{1/11} = 6.8$ and lines 1-3 relate to wave regimes with $\alpha = 0.8$, and lines 4-6 relate to $\alpha = 0.3$ (long waves which have at the limit a positive solitary wave). Lines 1, 4 in Fig. 3c relate to the value $R^{-1} = 0$; 1, 4 in Fig. 3d to 0.05; 2, 5 in Fig. 3c, d to 0.1; 3, 6 in Fig. 3c, d to 0.2.

We note some features of the behavior of the dependences for long waves (lines 4-6) presented in Fig. 3c, d. For them there are points of return $\mathrm{Re}_r(R^{-1})$ (dependences in Fig. 3 are provided after these points by broken lines), after which there may be degeneration into the corresponding wave of the first family of a triple period (lines 4-6 in Fig. 3c and 4, 5 in Fig. 3d) or a second point of return exists (line 6 in Fig. 3d) on reflection from which the dependence again goes into a region of high Reynolds numbers. Similar calculations for long waves with other values of α also show existence of return. For a fixed value of R^{-1} in plane (α, Re) the point of return forms several lines $\mathrm{Re}_*(\alpha)$. Depending on from which line the reflection occurs the wave may degenerate into the corresponding solution of the first family of double, triple, etc. spatial periods. Numerical calculation of these lines over a quite wide range of parameters Re and α is a difficult computation task and it is not performed in this work. With downflow over a vertical plane lines of returns are presented in [14].

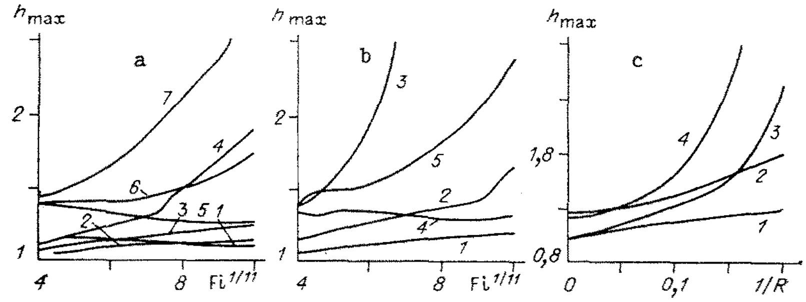

Fig. 4

For quite small values of R^{-1} (lines 1, 2, 4, 5 in Fig. 3c, lines 1, 4 in Fig. 3d) an increase in Re leads to an increase in wave amplitude as follows from Fig. 3c, d (sections of broken lines are not considered since their regimes are unstable). For values of R^{-1} relating to lines 3, 6 in Fig. 3c and 2, 3, 5, 6 in Fig. 3d an increase in Re leads to the reverse effect. With downflow over the inner surface of a cylinder of quite small radius with an increase in Re there is a critical increase in the maximum film thickness as follows from Fig. 3d.

Presented in Fig. 4a, b are dependences for maximum film thickness h_{max} on $Fi^{1/11}$ for downflow over a wire and over the inner surface of a cylinder. Here Re = 4, line 1 in Fig. 4a relates to a wave with $\alpha = 0.9$ with $R^{-1} = 0$, lines 2-4 in Fig. 4a and 1-3 in Fig. 4b relate to a wave with $\alpha = 1.0$ with $R^{-1} = 0.05$, 0.1, 0.2, respectively. Lines 5-7 in Fig. 4a and 4, 5 in Fig. 4b relate to waves with $\alpha = 0.32$ and 0.4 (long waves which have at the limit a positive solitary wave) with $R^{-1} = 0.05$, 0.1, 0.2, respectively.

It can be seen from Fig. 4a, b that depending on wall curvature an increase in $Fi^{1/11}$ may cause both an increase in wave amplitude (cylinder of small radius) and a reduction of it. In Figs. 4c and 5 the maximum film thickness h_{max} and some characteristic profiles of thickness as a function of cylinder radius are presented. Here Re = 4 and $Fi^{1/11} = 6.8$, lines 1, 2 in Fig. 4c relate to a wave regime with $\alpha = 1.0$ and 0.32 flowing over the outer surface of a cylinder, and lines 3, 4 in Fig. 4c relate to regimes with $\alpha = 1.0$ and 0.4 flowing over the inner surface of a cylinder. In Figs. 5a-c regimes with $\alpha = 0.4$ relate to downflow over the inner surface of a cylinder with $R^{-1} = 0.05$, 0.1, 0.15, respectively.

From the results presented in Figs. 4c and 5 it follows that an increase in curvature leads to an increase in wave amplitude. For downflow over an inner cylinder surface for each α there exists a value of radius R_{cr} which with approach toward it there is a very rapid increase in maximum thickness.

Thus, different wave regimes are considered for downflow of a thin layer of viscous liquid over the inner and outer surfaces of a vertical cylinder. Using the integral method a set of equations is obtained which describes the evolution of long-wave disturbances. It is shown that in the problem there are three external parameters: Re, Fi, and R^{-1}. The linear stability was studied for waveless downflow and quantitative conformity is demonstrated with similar results found on the basis of asymptotic expansion of the solutions of Navier–Stokes equations. Waveless downflow is unstable with all values of external parameters. Evolution of disturbances is governed by gravitational force (supply of energy), viscous forces (energy drainage), and forces of surface tension. It is shown that surface forces connected with wall curvature are destabilizing and tend to increase the deviation of the film from the average value in contrast to capillary forces which develop with longitudinal variations of film thickness. As a result of evolution steady-state traveling flow regimes may form which are also considered in this work. The main attention is devoted to the qualitative differences in the behavior of wave characteristics for flow regimes over a cylinder from similar dependences for flow over a vertical plane.

Calculations showed that for flow over the outer surface of a vertical cylinder there are at least two single-parameter wave families for which with fixed Re, Fi, and R^{-1} there is a wave number α. Waves of these families at the limit $\alpha \to 0$ are converted into a sequence of either negative or positive solitary waves.

For flow over the inner surface of a vertical cylinder the family which has at the limit a negative solitary wave exists with all values of external parameters, but a family which

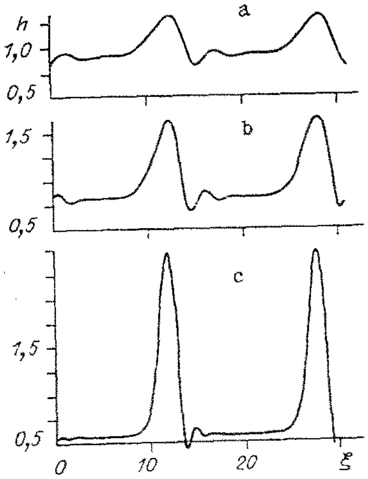

Fig. 5

has at the limit a positive wave only exists with relatively small amounts of wall curvature. For flow in a tube of quite small radius an effect is detected in calculations of a 'catastrophic' increase in amplitude of the established waves with advance into a region of instability for the smooth solution.

The effect is analyzed of all parameters on nonlinear wave characteristics and it is shown that depending on R^{-1} an increase in Re or a decrease in Fi may cause both strengthening of wave processes and a reduction of them, in contrast to downflow over a vertical plane where this led to an increase in wave amplitude. An increase in R^{-1} always intensifies wave processes.

LITERATURE CITED

1. S. V. Alekseenko, V. E. Nakoryakov, and B. G. Pokusaev, "Wave formation on a vertical falling liquid film," AIChE J., 31, No. 9 (1985).
2. V. E. Nakoryakov, S. V. Alekseenko, B. G. Pokusaev, and V. V. Orlov, "Instantaneous velocity profile in a wavy film of liquid," Inzh. Fiz. Zh., 33, No. 3 (1977).
3. P. Bach and J. Villadsen, "Simulation of the vertical flow of a thin wavy film using a finite-element method," Int. J. Heat Mass Transfer, 27, No. 5 (1984).
4. Yu. Ya. Trifonov and O. Yu. Tsvelodub, "Nonlinear waves in the surface of a liquid film falling over a vertical wall," Prikl. Mekh. Tekh. Fiz., No. 5 (1985).
5. Yu. Ya. Trifonov and O. Yu. Tsvelodub, "Stationary two-dimensional waves in a vertical falling film of liquid and their stability," Inzh. Fiz. Zh., 54, No. 1 (1988).
6. E. A. Demekhin and V. Ya. Shkadov, "Two dimensional wave regimes for a thin layer of viscous liquid," Izv. Akad. Nauk SSSR, Mekh. Zhidk. Gaza., No. 3 (1986).
7. V. E. Nakoryakov, B. G. Pokusaev, and S. V. Alekseenko, "Desorption of weakly soluble gas from falling wavy liquid films," in: Calculation of Heat Transfer in Energy-Chemical Processes [in Russian], IT SO Akad. Nauk SSSR, Novosibirsk (1981).
8. V. Ya. Shkadov, "Wave regimes for flow of a thin film of viscous liquid under the action of the force of gravity," Izv. Akad. Nauk SSSR, Mekh. Zhidk. Gaza., No. 1 (1967).
9. E. A. Demekhin, M. A. Kaplan, and R. A. Foigel', "Nonlinear waves in a falling viscous layer of magnetic liquid," Magn. Gidrodin., No. 1 (1988).
10. S. P. Lin and W. C. Liu, "Instability of film coating of wires and tubes," AIChE J., 21, No. 4 (1975).
11. P. L. Kapitsa and S. P. Kapitsa, "Wave flow of thin layers of viscous liquid," Zh. Éksp. Teor. Fiz., 19, No. 2 (1949).
12. V. Ya. Shkadov, "Solitary waves in a layer of viscous liquid," Izv. Akad. Nauk SSSR, Mekh. Zhidk. Gaza., No. 1 (1977).
13. A. V. Bunov, E. A. Demekhin, and V. Ya. Shkadov, "Nonidentical nature of a nonlinear wave regimes in a viscous layer," Prikl. Mat. Mekh., 48, No. 4 (1984).
14. Yu. Ya. Trifonov and O. Yu. Tsvelodub, "Branching of steady-state traveling wave regimes for a viscous film of liquid," Prikl. Mekh. Tekh. Fiz., No. 4 (1988).